

Temperature dependence of ODR range at 1550nm using 1D Binary and Ternary photonic crystals

SANJEEV SHARMA^{a*}, RAJENDRA KUMAR^b, Kh. S. SINGH^c, ARUN KUMAR^d

^aDepartment of Physics, GNCT College, Greater Noida, UP, India

^bDepartment of Physics, Gurukul Kangri Vishwavidyalaya Haridwar, Uttrakhand, India

^cDepartment of Physics, D. J. College Baraut Uttar Pradesh, India

^dAITEM, Amity University, Uttar Pradesh, India

Omni-directional photonic bandgaps (PBG) has been presented in the one-dimensional binary and ternary photonic crystals by using the semiconductor and dielectric materials layers of Si, SiO₂ and ZnS in the unit cell. The effect of temperature and angle of incidence on omnidirectional reflection (ODR) spectra of proposed structure for TE and TM polarization has also been studied. The PBG can be tuned by varying the temperature of the semiconductor material Si or by changing the angle of incidence. The ODR range can be increased by introducing the third layer of semiconductor materials in binary Photonic crystals. The existence of total Omni-directional reflection band gap at 1550 nm in 1D binary and ternary photonic crystal is predicted theoretically by using TMM method.

(Received March 14, 2016; accepted June 7, 2017)

Keywords: Photonic crystal, ODR, multilayered mirror

1. Introduction

The concept of photonic crystal structure was first introduced by E. Yablonoitch [1] and Sanjeev John [2] in 1987. In the past few years, photonic band gap structures attracted the attention of researchers [3–6], due to their enormous applications in optical communications, optoelectronics and optical instrumentation. These photonic band gap structures are multilayer structures formed by using two or more materials. These multilayered structures lead to formation of photonic band gaps or stop bands, in which propagation of electromagnetic waves of certain wavelengths are prohibited. However, these bands or ranges depend upon a number of parameters such as refractive indices of materials and angle of incidence. Also optical filters such as wavelength division multiplexer (WDM), DWDM, CWDM etc. can be designed by introducing defect layer between the alternate layers of photonic crystals [7-12]. Sanjeev et. al [7] design a single channel wavelength division multiplexer by using non linear photonic crystal and he found that the average change in central wavelength of defect mode is 0.08 nm/(GW/cm²).

The width of the OBGs plays an important role in the applications of 1DPC omnidirectional reflector. In recent years, one-dimensional ternary photonic crystals (1DTPCs) are also put forward to obtain the extended OBGs [13-16]. 1DTPCs are constituted by three material layers in a period of the lattice. Awasthi et al. [15] demonstrated that the wavelength range of OBGs can be enhanced by 108 nm when the structure was modified by sandwiching a thin layer of ZrO₂ between every two layers. When the sandwiched layer was CeF₃, the

enhancement in the range was 120 nm. Wu et al. [16] showed that the OBGs can be significantly enlarged in the ternary metal-dielectric PC. Xiang et al. [14] found that the zero-effective-phase bandgap will be enlarged by sandwiching the third material between the two single-negative materials.

In the present paper, we design a broad omnidirectional reflector (ODR) in one dimensional binary and ternary photonic crystal containing semiconductor and insulator layer. Also, the dielectric property of semiconductors depends not only on temperature but also on wavelength. Here we consider the binary semiconductor Si/SiO₂ and ternary semiconductor materials Si/SiO₂/ZnS multilayer system. The refractive index of SiO₂ and ZnS is independent of temperature and wavelength. But the refractive index of silicon layer is taken as a function of temperature and wavelength both [17, 18]. The semiconductor Si is depending on the temperature, it is possible to design thermally-tunable omnidirectional total reflector.

2. Theoretical model

The periodic structure consisting of alternate layers of refractive indices n_1 (first material layer), n_2 (second material layer) and n_3 (third material layer) with thicknesses d_1 , d_2 and d_3 respectively is depicted in Fig. 1. $d = d_1 + d_2 + d_3$ is the period of the lattice. It is assumed that the incident media is air ($n_0 = 1$). Light is incident on the multilayer at an angle θ_0 .

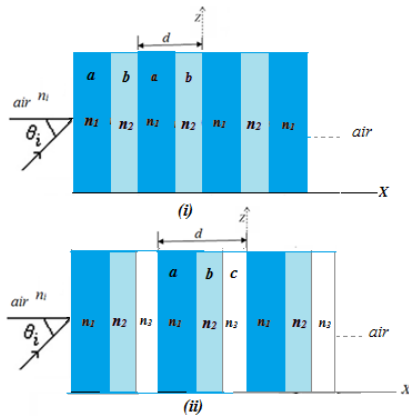


Fig. 1. Structure of one-dimensional (i) binary and (ii) ternary photonic crystals

Applying the transfer matrix method (TMM), the characteristic matrices for the TE and TM waves have the form [19, 20],

$$M[d] = \prod_{i=1}^k \begin{bmatrix} \cos \beta_i & -i \sin \beta_i \\ -ip_i \sin \beta_i & \cos \beta_i \end{bmatrix} = \begin{bmatrix} M_{11} & M_{12} \\ M_{21} & M_{22} \end{bmatrix} \quad (1)$$

where, $k = 2$ for binary photonic crystals and $k = 3$ for ternary photonic crystals (1, 2 and 3 signify the layers of refractive indices n_1 , n_2 and n_3 (respectively), $\beta_i = \frac{2\pi}{\lambda} p_i d_i \cos \theta_i$, $p_i = n_i \cos \theta_i$, θ_i is the ray angles inside the layer of refractive index n_i and is related to the angle of incidence θ_0 by

$$\cos \theta_i = \left[1 - \frac{n_0^2 \sin^2 \theta_0}{n_i^2} \right]^{\frac{1}{2}} \quad (2)$$

The total characteristic matrix of N -period of the structure given by,

$$M(d)^N \quad (3)$$

The reflection coefficient of the multilayer is given by,

$$r(\omega) = \frac{(m_{11} + m_{12}p_0)p_0 - (m_{21} + m_{22}p_0)}{(m_{11} + m_{12}p_0)p_0 + (m_{21} + m_{22}p_0)} \quad (4)$$

Where m_{ij} are the matrix elements and the reflectance for this structure can be written in the terms of reflection coefficient as,

$$R = |r(\omega)|^2 \quad (5)$$

Where, $p_0 = n_0 \cos \theta_0$

In binary photonic crystal we choose Si for material A, SiO_2 for material B and $N = 12$, so the proposed structure will be $[\text{air}/(\text{Si}/\text{SiO}_2)^{12}\text{Si}/\text{air}]$ and in ternary photonic crystal we choose Si for material A, SiO_2 for material B, ZnS for material C and $N = 12$, so the proposed structure will be $[\text{air}/(\text{Si}/\text{SiO}_2/\text{ZnS})^{12}\text{Si}/\text{air}]$.

The refractive indices of SiO_2 and ZnS are independent of temperature and wavelength. But the refractive index of silicon layer is taken as a function of both wavelength and temperature. The refractive index of silicon (Si) in the ranges 1.2–14 μm and 293–900K is represented as [17].

$$n^2(\lambda, T) = \varepsilon(T) + \frac{e^{-\frac{3\Delta L(T)}{L_{293}}}}{\lambda^2} (0.8948 + 4.3977 \times 10^{-4}T + 7.3835 \times 10^{-8}T^2) \quad (6)$$

Where,

$$\varepsilon(T) = 11.4445 + 2.7739 \times 10^{-4}T + 1.7050 \times 10^{-6}T^2 - 8.1347 \times 10^{-10}T^3$$

and thermal expansion [16]

$$\frac{\Delta L(T)}{L_{293}} = -0.021 - 4.149 \times 10^{-7}T - 4.620 \times 10^{-10}T^2 + 1.482 \times 10^{-11}T^3 \quad (7)$$

for $293\text{K} \leq T \leq 1600\text{K}$

The thermal coefficient of silicon is $2.6 \times 10^{-6}/\text{K}$ [17]. In the thickness of Si layer, the effect of thermal expansion has been taken by applying following equation:

$$d_1(T) = d_{293} + \left(1 + \frac{\Delta L(T)}{L_{293}} \right) \quad (8)$$

3. Result and discussion

In this paper, we have presented the omnidirectional reflection spectra of one-dimensional binary and ternary photonic crystals. The refractive indices of SiO_2 and ZnS are independent of temperature and wavelength. But the refractive index of silicon layer is taken as a function of both wavelength and temperature. Here, we have chosen the refractive index range of silicon (Si) from 1.2–3.3 μm and temperature range from 300–1200K. The plot of the refractive index as the function of wavelength and temperature is shown in Fig. 2. From Fig. 2, it is clear that the refractive index of silicon layers increases with temperature.

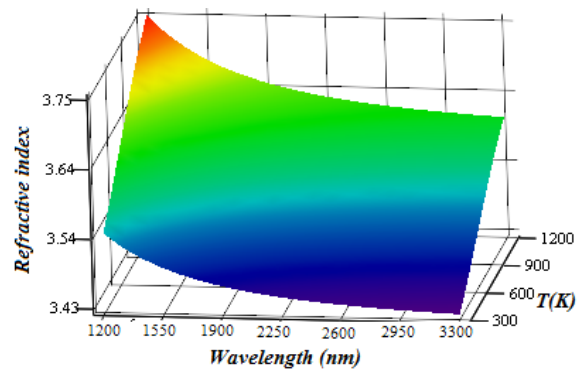


Fig. 2. Refractive index as a function of wavelength and temperature

For our calculations we studied two different structures of binary and ternary one-dimensional photonic crystals namely –

Structure I: Si/SiO₂ one-dimensional binary photonic crystal

Structure II: Si/SiO₂/ZnS one-dimensional ternary photonic crystal

The refractive indices of SiO₂ and ZnS are 1.45 and 2.27 respectively [22-23]; and the refractive index of Si is dependent of both temperature and wavelength. Applying transfer matrix method, we plotted reflectance of the structures with wavelength for various angles of incidence. In structure I, we have taken the thicknesses of Si and SiO₂ layers to be $a = 155$ nm, $b = 250$ nm and $d = a + b = 405$ nm. And for structure II, we have taken the thicknesses of Si, SiO₂ and ZnS layers to be $a = 155$ nm, $b = 250$ nm, $c = 20$ nm and $d = a + b + c = 425$ nm. This particular combination of thickness of Si, SiO₂ and ZnS layers has been chosen such that ODR range in the reflection spectra of such a structure can be observed. Fig. 3 & Fig. 4 show the reflectance of the structure for the variation of refractive index profile of Si materials for different temperature (300K and 1200K) and different

angles of incidence, namely, 0°, 45° and 85° for TE and TM mode respectively and the ODR range for angles of incidence from 0° to 85° is shown in the shaded portion of Fig. 3 and Fig. 4.

From the plots of reflection spectra of **Structure I (Si/SiO₂)** for different angles of incidence, the 100 percent reflection ranges for different angles of incidence at Temperature 300K & 1200K are tabulated in Table 1. It is clear from Table 1 that the total Omnidirectional range (ODR) of wavelength for this multilayer structure lies between 1450–1865 nm at $T = 300$ K and the width of the omnidirectional wavelength range is **415 nm** and at $T = 1200$ K the omnidirectional range lies between 1485–1955 nm and the width of the Omnidirectional wavelength range is **470 nm**. It is clear that when we increase the angle of incidence (at constant temperature) the bandgap shift towards the shorter wavelength region. On the other hand as we increase the temperature (at a constant angle of incidence) the bandgaps shift towards the longer wavelength region which is shown in Fig. 5. Now in structure II, we will discuss how to extend the wavelength range of omnidirectional bandgap in one-dimensional ternary photonic crystal (1DTPC).

Table 1. Photonic bandgap structure of binary PC as a function of Temperature and angle of incidence

Temperature T(K)	Angle of incidence (θ)	TE (nm)	Band width (nm)	TM (nm)	Band width (nm)
300	0	1450-2437	987	1450-2437	987
	45	1352-2375	1023	1405-2170	765
	85	1243-2323	1080	1352-1865	513
1200	0	1485-2550	1065	1485-2550	1065
	45	1392-2493	1101	1445-2282	837
	85	1290-2435	1135	1390-1955	565

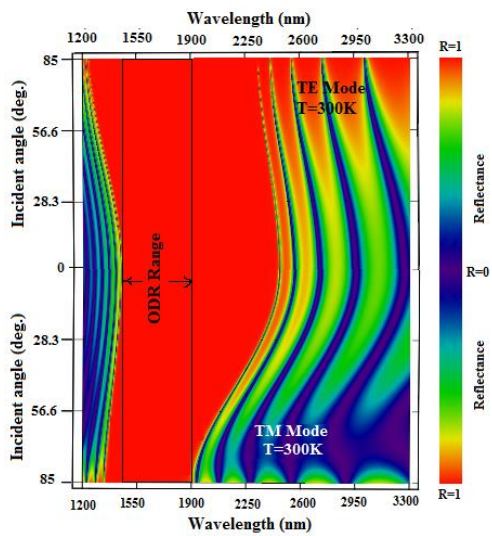


Fig. 3. Omnidirectional reflection (ODR) spectrum of 1D binary photonic crystals (Si/SiO₂) at different angle of incidence at $T=300$ K.

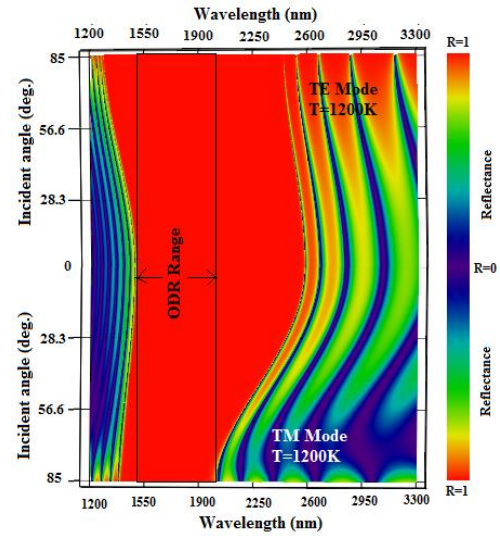


Fig. 4. Omnidirectional reflection (ODR) spectrum of 1D binary photonic crystals (Si/SiO₂) at different angle of incidence at $T=1200$ K.

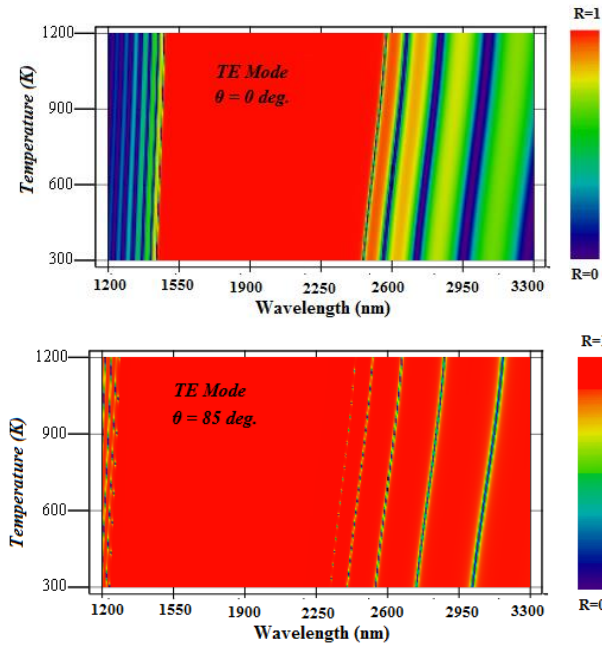


Fig. 5. Reflectance spectra of 1D binary photonic crystal as a function of wavelength and temperature

Table 2. Photonic bandgap structure of ternary PC as a function of Temperature and angle of incidence

Temperature T(K)	Angle of incidence (θ)	TE (nm)	Band width (nm)	TM (nm)	Band width (nm)
300	0	1512-2545	1033	1512-2545	1033
	45	1407-2482	1075	1465-2273	808
	85	1293-2423	1130	1412-1982	570
1200	0	1545-2667	1122	1545-2667	1122
	45	1442-2600	1158	1505-2382	877
	85	1320-2625	1305	1450-2075	625

From the plots of reflection spectra of **Structure II** (Si/SiO₂/ZnS) for different angles of incidence, the 100 percent reflection ranges for different angles of incidence at Temperature 300K & 1200K are tabulated in Table 2. It is clear from Table 2 that the total omnidirectional range (ODR) of wavelength for this multilayer structure lies between 1512–1982 nm at T = 300K and the width of the Omnidirectional wavelength range is **470 nm** and at T = 1200K the omnidirectional range lies between 1545–2075 nm and the width of the omnidirectional wavelength range is **530 nm**. It is clear that when we increase the angle of incidence (at constant temperature) the bandgap shift towards the shorter wavelength region. On the other hand as we increase the temperature (at a constant angle of incidence) the bandgaps shift towards the longer wavelength region which is shown in Fig. 6.

Hence, each of these two multilayered one-dimensional structures can be used as an omni-directional mirror in optical communication devices. However, Structure II has the broadest ODR range of wavelength. In the two structures considered in this paper, we have chosen the parameters of each of the structures such that the 1550 nm wavelength which is third transmission window primarily used in optical communication falls in

the omnidirectional reflection ranges of wavelength for these structures.

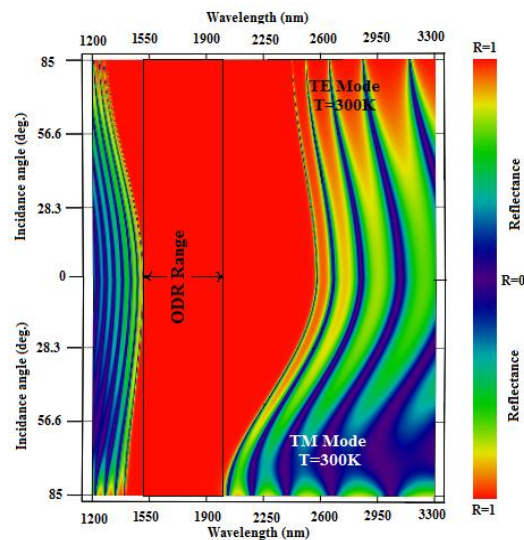


Fig. 6. Omnidirectional reflection (ODR) spectrum of 1D ternary photonic crystal (Si/SiO₂/ZnS) at different angle of incidence at T=300K

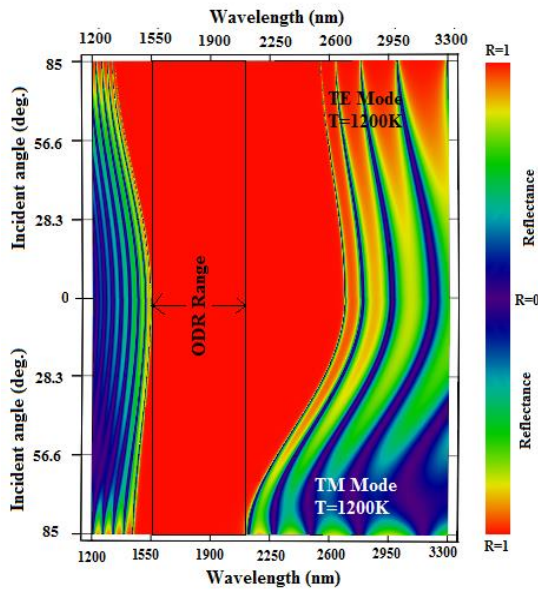


Fig. 7. Omnidirectional reflection (ODR) spectrum of 1D ternary photonic crystal (Si/SiO₂/ZnS) at different angle of incidence at T=1200K

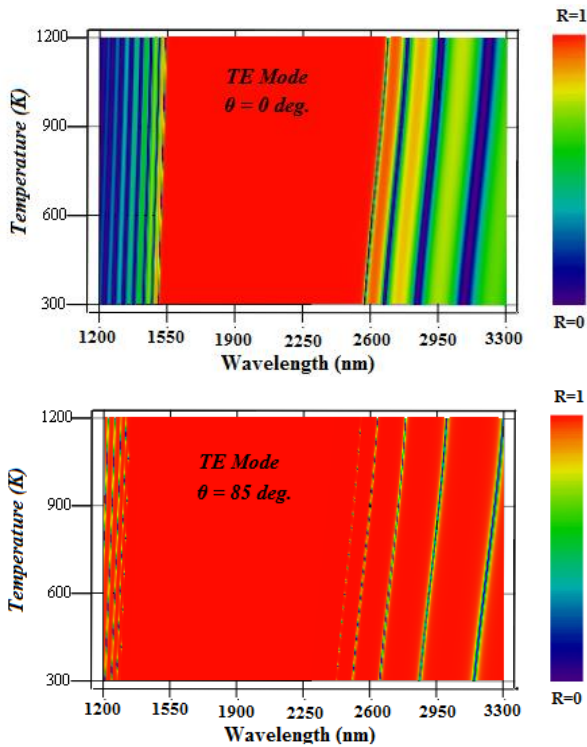


Fig. 8. Reflectance spectra of 1D ternary photonic crystal as a function of wavelength and temperature

In comparison with the omnidirectional bandwidth in the one dimensional binary photonic crystal (1DBPC), it is seen that the omnidirectional bandwidth in the 1DTPC is about **55 nm** larger than that without introducing semiconductor layer in the 1DBPC at temperature T=300K. And the omnidirectional bandwidth in the 1DTPC is about **60 nm** larger than that without introducing semiconductor layer in the 1DBPC at temperature

T=1200K. Hence, it is very effective method to design a broad omnidirectional OBG in the 1DTPC by sandwiching the semiconductor layer between two dielectric and semiconductor layer in the unit cell.

4. Conclusion

In this paper, we have designed a new type of broad omnidirectional and thermally tunable PBGs in one-dimensional binary and ternary photonic crystals composed of the semiconductor and dielectric materials. The angle and temperature dependence of these PBGs have been investigated. It is found that the bandgap width of these omnidirectional PBGs can be enhanced by introducing the additional semiconductor layer within binary photonic crystal material layers.

It is seen that the omnidirectional bandwidth in the 1DTPC is about **55 nm** larger than that without introducing semiconductor layer in the 1DBPC at temperature T=300K and the omnidirectional bandwidth in the 1DTPC is about **60 nm** larger than that without introducing semiconductor layer in the 1DBPC at temperature T=1200K. The variation of reflectance for both binary and ternary photonic crystal can be used as omnidirectional reflectors in fiber optic communication systems which fall in the wavelength range around 1550 nm (third transmission window). Such broad omnidirectional and thermally tunable PBGs will offer many prospects for omnidirectional mirrors, temperature sensing device, optical filters, polarizer, and other optical devices of optical communications in the future.

Acknowledgment

One of the authors S. Sharma is thankful to the Head, department of physics, Gurukul Kangri Vishwavidyalaya Haridwar, Mr. Pratap Singh Sahrawat, Department of Electronics, GNCT Greater Noida and Head, department of Physics, D.J. College Barout (UP) for their kind co-operation.

References

- [1] E. Yablonovitch, Phys. Rev. Lett. **58**, 2059 (1987).
- [2] S. John, Phys. Rev. Lett. **58**, 2486 (1987).
- [3] X. Wang, X. Hu, Y. Li, W. Jia, C. Xu, X. Liu, J. Zi, Appl. Phys. Lett. **80**, 4291 (2002).
- [4] Fang-Cao Peng, Ming-Yu Jiang, Jain Weiwu, Optoelectron. Adv. Mat. **11**, 12 (2017).
- [5] Sanjeev Sharma, Rajendra Kumar, Kh. S. Singh, Arun Kumar, Vipin Kumar, Optik- Int. Journal of light and electronic optics **126**, 1146 (2015).
- [6] Ji-Jang Wu, Jin-Xia Gao, Material Chemistry and Physics (Elsevier) **171**, 91 (2016).
- [7] Sanjeev Sharma, Rajendra Kumar, Kh. S. Singh, Vipin Kumar, Arun Kumar, J. Optoelectron. Adv. M. **16**(9-10), 1015 (2014).

- [8] Rajandeep Singh, Maninder Lal Singh, Optoelectron. Adv. Mat. **10**, 619 (2016).
- [9] Harkiranjeet Kaur, Rajinder Singh Kaler, Balveer Painam, Optoelectron. Adv. Mat. **11**, 23 (2017).
- [10] Zhaoming Luo, Min Chen, Jiyuan Deng, Ying Chen, Jing Liu, Optik- Int. Journal of light and electronic optics, **127**(1), 259 (2016).
- [11] R. Talebzadeh, M. Soroosh, J. Optoelectron. Adv. M. **17**(11-12), 1593 (2015).
- [12] H. Alipour-Banaei, S. Serajmohammadi, F. Mehdizadeh, J. Optoelectron. Adv. M. **17**(3-4), 259 (2015).
- [13] A. Banerjee, Progress In Electromagnetics Research, **89**, 11 (2009).
- [14] Y. Xiang, X. Dai, S. Wen, Z. Tang, D. Fan, Appl. Phys. B **103**, 897 (2011).
- [15] S. K. Awasthi, U. Malaviya, S. P. Ojha, J. Opt. Soc. Am. B **23** 2566 (2006).
- [16] C.-J. Wu, Y.-H. Chung, B.-J. Syu, T.-J. Yang, Progress In Electromagnetics Research **102**, 81 (2010).
- [17] H. H. Li, J. Phys. Chem. Ref. Data **9**, 561 (1980).
- [18] Vipin Kumar, B. Suthar, Arun kumar, Kh. S. Singh, A. Bhargava, Physica B **416**, 106 (2013).
- [19] P. Yeh, Wiley: New York, **118** (1988).
- [20] P. Yeh, A. Yariv, C. S. Hong, Journal of the Optical Society of America, **67**(4) 423 (1977).
- [21] Y. S. Touloukian, R. K. Kirby, R. E. Taylor, T. Y. R. Lee, New York, 13, 1977.
- [22] D. G. Drummond, Proc. R. Soc. London **153**, 328 (1935).
- [23] J. R. DeVore, J. Opt. Soc. Am. **41**, 416 (1951).

*Corresponding author: sanjeevsharma145@gmail.com